

05,08

## Mechanisms of ultrafast demagnetization and reverse spin Hall effect in cobalt-based terahertz thin-film emitters

© M.S. Lapteva, A.V. Gorbatova, P.Yu. Avdeev, E.D. Lebedeva, E.S. Shahurin,  
A.A. Klimov, A.M. Buryakov

MIREA — Russian Technological University,  
Moscow, Russia

E-mail: lapteva@mirea.ru, buryakov@mirea.ru

Received April 18, 2024

Revised April 18, 2024

Accepted May 8, 2024

The effect of the cobalt layer thickness on the magnetic characteristics in a series of spintronic terahertz emitters is analyzed. Both single-layer  $\text{Co}(d)$  films, where  $d$  is a variable thickness from 3 to 10 nm, and two-layer structures of  $\text{Co}(d)/\text{W}(3 \text{ nm})$  and  $\text{W}(3 \text{ nm})/\text{Co}(d)$  with uniaxial magnetic anisotropy are considered. The results emphasize the critical role of structural parameters, especially in thin layers, where an increase in magnetic stiffness and coercive field is observed due to an increase in the density of defects at the interfaces. It is shown that optimal magnetic characteristics and energy efficiency are achieved in ferromagnetic films with a thickness of about 10 nm, which is important for the development of THz emitters with high polarization controllability. The study demonstrates that the structure of  $\text{Co}(10 \text{ nm})/\text{W}(3 \text{ nm})$  provides a better balance between the efficiency of THz emission and the coercive field, due to a combination of mechanisms of ultrafast demagnetization and the reverse spin Hall effect

**Keywords:** ultrafast demagnetization, spin-charge conversion, reverse spin-Hall effect, terahertz radiation, spintronic emitter, magnetron sputtering, cobalt.

DOI: 10.61011/PSS.2024.07.58974.45HH

### 1. Introduction

THz spintronics in recent years has demonstrated significant achievements having offered the brand new approaches to efficient generation of THz-emission via a superfast control of magnetization and spin dynamics in thin ferromagnetic (FM) and FM/nonmagnetic (NM) metallic films. Special attention was paid to the films with thickness of several nanometers where these processes are clearly manifested. The key breakthrough in this area was achieved by Kampfrath group in 2013 [1], that was first to demonstrate a spintronic THz-emitter functioning based on the inverse spin Hall effect. This discovery provided new opportunities for creation of simple and high-energy THz-emission sources generating intensive and wideband (up to 10 THz) THz-emission pulses comparable with organic crystals in terms of peak electrical fields [2,3]. The concept of spintronic THz-emitter itself allows to control the polarization of THz-emission due to the change of orientation of ferromagnetic layer magnetic moment [4]. Due to these features the spintronic THz-emitters are distinguished among the variety of THz-sources and become perspective for use in a wide range of applications, from biomedicine to telecommunications.

Since the spintronic THz-emitters have been discovered a lot of efforts were made for their improvement to reach the most efficient THz-generation. The main strategy for improvement is based on solving the following tasks: 1) selection of the best materials, 2) improvement of their thicknesses. An overview summarizing major achievements

in this area for the last 10 years is given in paper [3] Not only a wide range of ferromagnetic materials used as a spin current source are considered here, but also a wide group of materials that can be used for transformation of the spin current into charge current. Materials used in THz spintronic emitters for a spin-charge transformation are featuring a wide range of various properties and include: heavy non-magnetic metals [3,5] and magnets [4], including anti-ferromagnetic materials [6–8] with high value of Hall spin angle, topological insulators [9–12] and semiconductors [13–18].

When it comes to the analysis of metal layers thickness influence on THz-emission efficiency, also many studies have been performed [5,19–21]. The correlation between the thickness of FM- and NM-layers and amplitude of the generated THz-wave in classic spintronic emitters based on the inverse spin Hall effect are analyzed in details in paper [19]. Complying with the model presented in paper [19] when selecting the metal layers thickness it is necessary to strike a compromise between three basic parameters [19]: 1) optical power  $P_{abs}$  absorbed by the structure and directly influencing the value of generated THz-field 2) critical thickness of FM-layer  $d_0$  ( $\sim 0.8 \text{ nm}$  for iron) defining the spin current generation threshold for its further transport to HM-layer and, hence, defining the initial THz-generation threshold, 3) parameter characterizing exponential attenuation of THz-signal when passing through metal layers and determining the reverse ratio of THz-intensity versus total thickness of spintronic emitter.

Parameters of the fabricated group of samples

| Sample description | Layer thickness, nm        | $H_c$ (E.A.), Oe<br>[MOKE]/[THz] | $H_c$ (H.A.), Oe<br>[MOKE]/[THz] |
|--------------------|----------------------------|----------------------------------|----------------------------------|
| Co(10 nm)/W(3 nm)  | $10.0 \pm 1.5/3.1 \pm 0.5$ | 56/41                            | 19/22                            |
| Co(5 nm)/W(3 nm)   | $5.2 \pm 0.3/3.3 \pm 0.2$  | 106/70                           | 40/47                            |
| Co(3 nm)/W(3 nm)   | $3 \pm 0.3/3 \pm 0.1$      | 141/84                           | 65/62                            |
| W(3 nm)/Co(10 nm)  | $3 \pm 0.1/10.1 \pm 0.1$   | 57/32                            | 2/28                             |
| W(3 nm)/Co(5 nm)   | $3.3 \pm 0.2/5.3 \pm 0.3$  | 37/37                            | 22/22                            |
| W(3 nm)/Co(3 nm)   | $3 \pm 0.01/2.9 \pm 0.1$   | 95/79                            | 1/63                             |
| Co(10 nm)          | $11.6 \pm 1.0$             | 63/46                            | 63/48                            |
| Co(5 nm)           | $4.9 \pm 0.3$              | 229/199                          | 157/137                          |
| Co(3 nm)           | $3.5 \pm 0.3$              | 181/169                          | 110/98                           |

As it comes to THz-emission polarization control, the design of a inter-plane magnetic anisotropy with a clearly defined hard magnetic axis during emitters fabrication is of the key importance [4,22–27]. However, in spite of extensive research in this area, small attention was paid to the influence of structural characteristics of thin FM-films and their interfaces on magnetic properties which, in their turn, are a key factor for THz-polarization control. Only in paper [19] a small analysis was performed of spintronic Fe/Pt emitter's magnetic characteristics which are critical for THz-polarization control. The authors demonstrate that with FM-layer thicknesses of several nanometers the structure is characterized by a magnetic loop, corresponding to the easy magnetic axis and with decrease of Fe ferromagnetic layer below the critical value  $d_0$  the structure behavior tends to be super-magnetic.

In this paper we focus on the analysis of influence of ferromagnetic Co layer thickness on magnetic characteristics and efficiency of THz-emission generation in a series of spintronic emitters, including Co/W and W/Co structures with a fixed 3 nm thickness of HM-layer. Our main task is to define how the FM-layer thickness variation impacts the key parameters of THz-emitters.

## 2. Experiment description

In this paper we considered three series of samples of spintronic THz-emitters: single-layer films of Cobalt, two-layer FM/NM structures, where Co was used as a ferromagnetic material, and W as a normal metal. We analyzed two types of two-layer structures differed by the order of layers sequence: W/Co( $d$ ) and Co( $d$ )/W. Thin films of emitters were fabricated by the method of magnetron sputtering using DST-3A (VacCoat) system on SiO<sub>2</sub> substrates in the outer magnetic field with intensity of  $H_{\text{ext}} = 3.5$  kOe for generation of a inter-plane uniaxial magnetic anisotropy. The pressure in the chamber before deposition was  $10^{-5}$  Torr. The films were sputtered at room temperature in argon environment. Argon pressure during deposition of all samples was  $9.7 \cdot 10^{-3}$  Torr, power of RF-source — 210 W for Co and 150 W for W. In the

fabricated series of samples the thickness of Co films was 3, 5 and 10 nm. Thickness of non-magnetic layer W was constant — 3 nm. Description of manufactured samples is given in Table.

Analysis of magnetic characteristics (saturation field, anisotropy field and coercive force) of the fabricated structures was carried out using standard method of meridional magneto-optic Kerr effect (MOKE) along the structure magnetization axis relative to the incident light on the sample. Also the films surface characteristics were analyzed by method of atomic-force microscopy (AFM). The roughness measurements for a fabricated series of structures didn't allow to identify the influence of FM-layer thickness on the roughness parameters. The values of average roughness ( $R_a$ ) corresponded to  $0.647 \pm 0.2$  nm, while root-mean-square roughness value ( $R_q$ ) was  $1.037 \pm 0.4$  nm for all analyzed films.

Within THz-emission study the standard method of terahertz emission spectroscopy with time resolution was used (THz-TDS). Ti:Sapphire femtosecond laser with wavelength 800 nm, pulse frequency 3 kHz and duration of about 35 fs was used as a source of excitation emission. To study the influence of magnetic field on generation of THz-emission the sample was placed in constant magnetic field generated by an electromagnet. The system and THz-emission recording method are given in details in our papers [4,28].

## 3. Results and discussion

The thicknesses of metal films in a series of spintronic emitter samples were confirmed by the method of ellipsometry. The results of layers thickness measurements are given in the Table. The loops of magnetic hysteresis in „hard“ magnetic axis and „easy“ magnetic axis obtained by MOKE method are given in Figure 1 The analysis of measurements results identified the increase of coercive field  $H_c$  with the decrease of Co ferromagnetic layer. Specific values  $H_c$  for each sample are given in the Table.

From Figure 1 we can see that magnetic hysteresis loops obtained by MOKE method and THz-hysteresis loops for

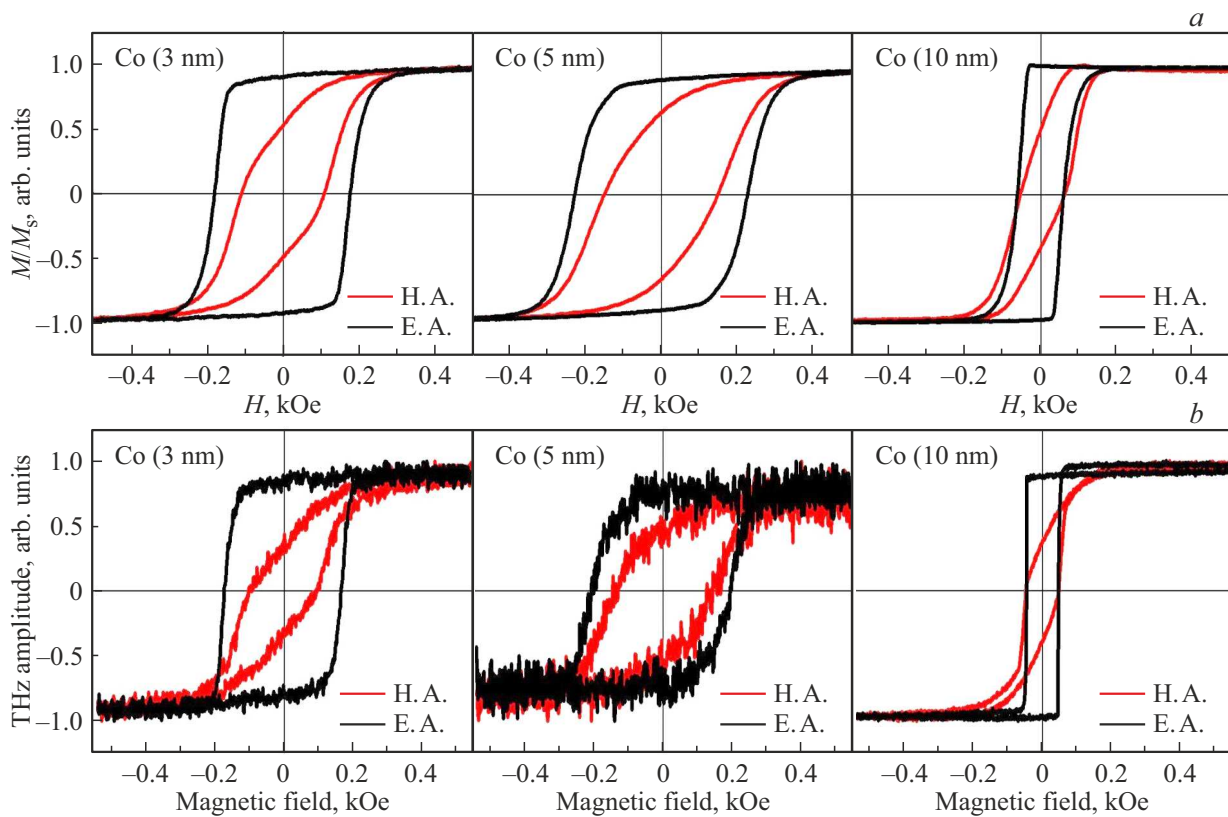


**Figure 1.** Magneto-optical hysteresis (a) and magnetic THz-hysteresis (b) for Co films, 3, 5 and 10 nm.

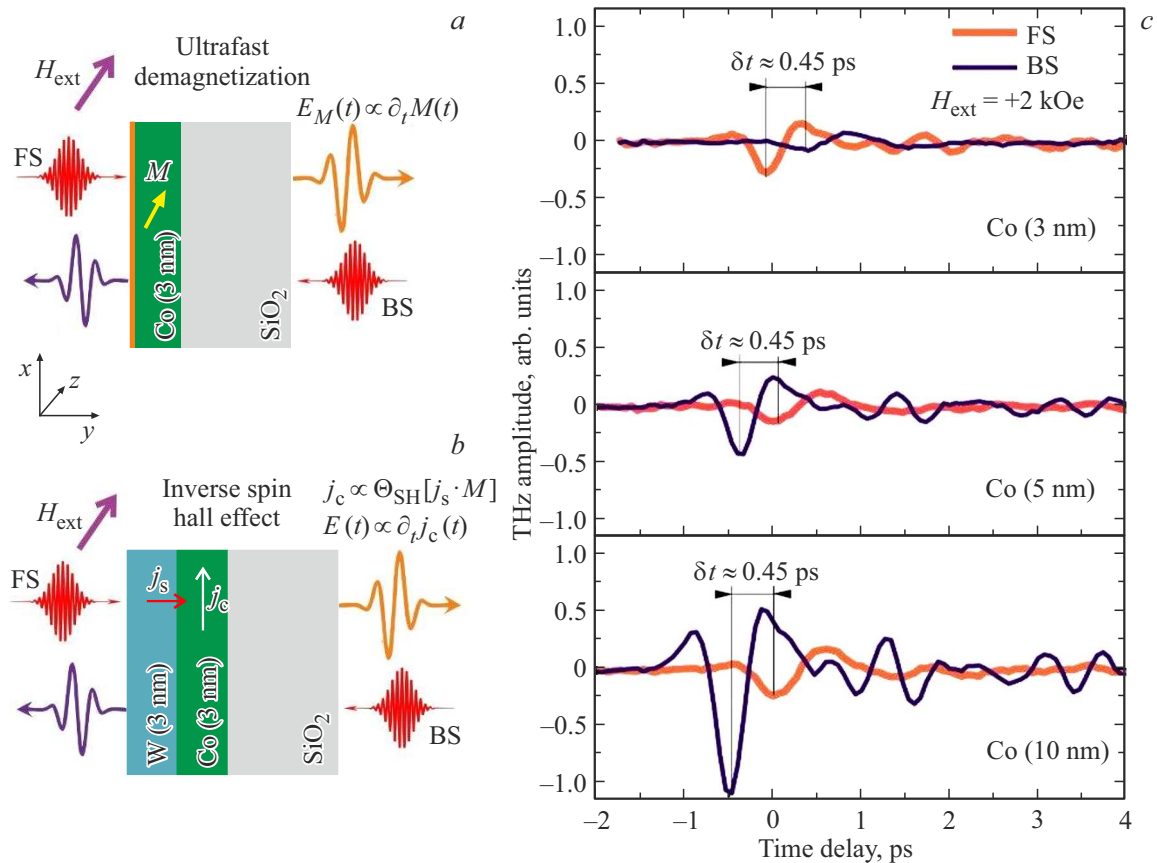
a series of Co-based structures coincide in terms of all ferromagnetic metal thicknesses. As we may see from the obtained loops the reduction of Co thickness is accompanied by the growth of coercive field  $H_c$ , which is clearly observed both, for the MOKE-loops, and for magnetic THz-hysteresis loops. The results of the study proved existence of a distinct magnetic anisotropy with clearly defined hard and easy magnetic axes which is crucial for control of THz-emission polarization. All data  $H_c$  obtained from analysis of the loops are given in the Table.

Figure 2 schematically shows the samples of ferromagnetic Cobalt film spintronic emitters studied in this paper (Figure 2, a) and FM/NM bi-layers with W/Co as an example (b). For these two types of THz-generators the THz-generation mechanism will be different. In the first case the THz-generation occurs due to the process of superfast demagnetization in the ferromagnetic layer, in the second case — due to the process of spin-charge transformation as a result of inverse spin Hall effect. Figure 3, c illustrates the temporal dynamics of THz-signal for single-layer 3, 5 and 10 nm thick Cobalt samples measured in magnetic field +2 kOe for two sample orientations relative to the magnetic field propagation direction: FS — when the structure is irradiated from the side of magnetic films, BS — when the structure is irradiated from the substrate side. Time delay between THz-signals, measured in FS and BS geometries, occurs because of difference in the refraction indices fro

optical ( $n = 1.4526$ ) and THz-emissions ( $n \approx 2.127$ ) in the substrate  $\text{SiO}_2$ . The difference in THz-signal amplitude for the two orientations is explained by different absorption of THz-emission in the glass substrate. As seen from Figure 3, c the change of the sample orientation with respect to the laser beam for FS and BS configurations is not followed by inversion of THz-signal phase which is the case for superfast demagnetization.

For bi-layer FM/NM structures the phase of THz-signal will be defined not only by the direction of applied outer magnetic field which defines the direction of magnetic moment in cobalt film but by the direction of spin current flow as well. The direction of the spin current flow in such structures, in its turn, will depend on the change of the sample orientation. Figure 3, a illustrates the temporal dynamics of THz-signals obtained for W(3 nm)/Co(5 nm) and Co(5 nm)/W(3 nm) samples in the outer magnetic field +2 kOe oriented parallel to the easy axis. As seen from Figure 3, a, the change of FS sample configuration into BS (see Figure 2, b) will result in the change of terahertz pulse polarity. The change of THz-signal phase when transiting from the front side to the reverse side in FM/NM like structures is a confirmation of the spin effect contribution into THz-emission generation.

The results shown in Figure 3, b, demonstrate the influence of Co layer in Co/W structures on THz-hysteresis when the magnetic field is applied along H.A. (top) and E.A. (bot-



**Figure 2.** (a) The scheme of THz-emission generation in case of superfast demagnetization in Cobalt ferromagnetic films. (b) Spin-charge transformation in case of Hall inverse effect in a classic spintronic W/Co emitter. (c) Temporal dynamics of THz-signal generated by a series of simple emitters on the basis of Cobalt films 3, 5 and 10 nm thick, measured in the outer magnetic field +2 kOe in FS and BS configurations.

tom), respectively. With the growth of Cobalt thickness a distinct decrease of the coercive field is observed, as in the case of Co single-layer spintronic emitters (Figure 1). The decrease of coercive field with the growth of ferromagnetic film thickness is a result of a complex interaction between the domain structure, magnetic interactions in the material and structural characteristics of the film. The magnet domains in thin films are distinguished by small sizes and a more complex structure because of high surface energy compared to the thick films, which is accompanied by a much higher magnetic hardness. With the growth of the ferromagnetic material the size of domains also increases which makes the process of their re-magnetization easier and, hence, reduces the coercive field. Moreover, in very thin films the defects, especially at the interfaces, as well as at the grain boundaries, may also lead to higher coercivity, while in the thick films the stresses may be distributed more evenly, making their re-magnetization process easier. In particular, in case of bi-layer Co/W spintronic emitters, the coercive field for the sample with 3 nm thick Cobalt is 84 Oe and it decreases twofold up to 41 Oe when the sample thickness reaches 10 nm, which proves the trend of coercivity decrease with the layer thickness growth.

Figure 4 illustrates the result of THz-generation efficiency in the studied structures where THz-emission generation occurs due to superfast demagnetization processes (single-layer Co films emitters and double-layer Co/W(3 nm)) structures and inverse spin Hall effect (W(3 nm)/Co), depending on the ferromagnetic layer thickness. The amplitude of THz-signals, shown in Figure 4, is calculated as a sum of maximal and minimal values of THz-signal (Peak-to-Peak amplitude), which corresponds to the full amplitude of a single THz-pulse oscillations.

For W/Co structure the amplitude of THz-signal drops evenly with the increase Co layer thickness, which is consistent with results in other papers [5,19–21]. Such behavior is predictable, given the model presented in paper [19], where dependence of generated THz-signal from the layer thickness in ferromagnetic and non-magnet materials is described.

For the single-layer Co and Co/W samples described earlier in this paper it was demonstrated that super-fast demagnetization in such structures is the basic (prevailing for Co/W) mechanism of THz-emission generation, which is also in line with other papers, e.g. for Cobalt [29]. The growth of THz-signal amplitude in these emitters with the

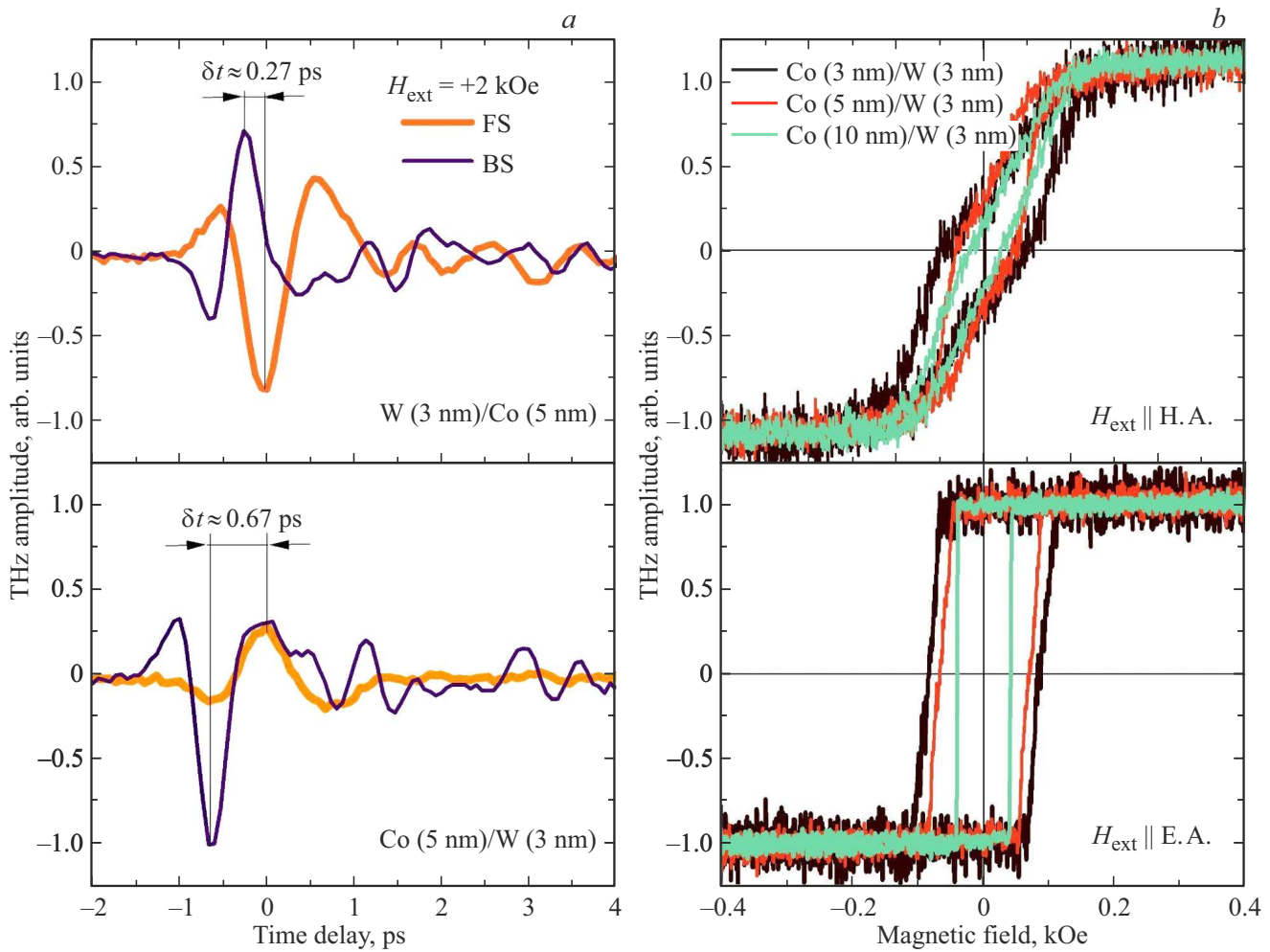


**Figure 3.** (a) Temporary profiles of terahertz signal for W/Co and Co/W structures for BS and FS configurations obtained in magnetic field +2 kOe. (b) Magnetic THz-hysteresis obtained for structures Co(3,5,10 nm)/W(3 nm) during magnetization along H.A. and E.A.

growth of thickness of ferromagnetic film is associated with the increase of inter-plane magnetization component in the Cobalt layer as its thickness grows [29]. Here we rely on the assumption that an optical pumping pulse coherently excites the elemental magnetic dipoles causing the change of magnetization with time and leading to generation of electrical field emitted in the far zone and polarized in  $x$  direction, where  $E_x(t)$  is proportional to  $M_x$ ,  $x$  — a component of the ferromagnetic layer magnetization vector.

The inverse relation between THz-emission and Cobalt layer thickness in the series of Co/W samples is somewhat an unexpected case since, as mentioned earlier, the mechanism of THz-emission generation shall be related to the inverse spin Hall effect. However, monotonous growth of THz-emission amplitude with the growth of Co layer thickness for this sample indicates a prevailing role of super-fast demagnetization in the mechanism of THz-generation. At the same time, the results shown in Figure 3 for Co(5 nm)/W(3 nm) sample prove that THz-signal is inverted due to a change in the charge current flow direction for FS and BS configurations which is consistent with the

inverse spin Hall effect. Thus, we may conclude that for Co/W samples the THz-emission generation includes simultaneously two mechanisms: super-fast demagnetization and spin-charge transformation due to the inverse spin Hall effect, the first mechanism being prevailing which is seen from the ratio of THz-signal amplitude versus Cobalt layer thickness (Figure 4). This, in its turn, explains the higher value of THz-amplitude compared to the pure Cobalt films as seen in Figure 4.

Magnetic hysteresis loops studied for thicknesses of Cobalt layers of 3 and 5 nm (Figure 3, b) show a significant increase in coercive field as expected because of such inhomogeneities as surface roughness of Cobalt film and other structural defects peculiar to the thin films. It was found that the thinnest Co film of 3 nm among Co/W samples, where the impact of surface effects is maximal, demonstrates the lowest amplitude of THz-emission, thus, indicating the influence of the micro-structural characteristics on the emission efficiency.

Summarizing all the above, it shall be emphasized that the most perspective structures for creation of THz-emitters

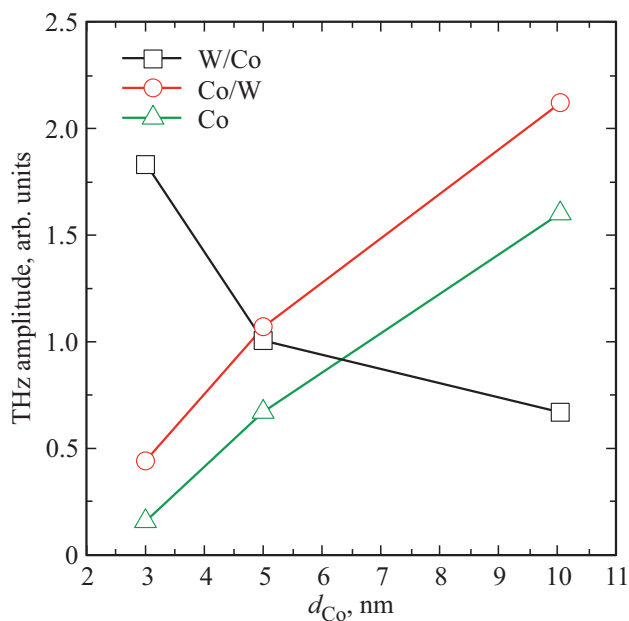


**Figure 4.** Efficiency of THz-generation depending on Co layer thickness in W/Co, Co/W and Co structures.

with controlled polarization are the structures like Co (10 nm)/W(3 nm). This configuration is featuring high amplitude of THz-emission comparable with those observed in classic double-layer thin-film W(3 nm)/Co(3 nm) emitters operating based on the inverse spin Hall effect. In addition, the Co(10 nm)/W(3 nm) structure outpaces the thin-film layers of Cobalt in terms of efficiency of THz-emission which is in favor of the use of complex multi-layer systems compared to the single-layer ones which rely on the super-fast demagnetization effect only. Thus, the results of our study focus on the importance of ferromagnetic films structural singularities to be taken into account in development and improvement of spintronic THz-emitters with a purpose to provide THz-emission polarization control.

#### 4. Conclusion

This paper outlines the study of a series of THz-emitters based on thin Cobalt films of various thicknesses (3, 5, and 10 nm): Co, W(3 nm)/Co and Co/W(3 nm). A detailed analysis of THz-generation mechanisms in these structures allowed to identify that in the single-layer Co films the generation of THz-emission is closely related to the process of super-fast demagnetization. This was proved by observing the increase of THz-emission intensity with the growth of Cobalt thickness, as well as by the absence of dependence of THz-signal phase from the direction of structure irradiation by laser pulse. In double-layer W/Co structures, functioning based on the inverse spin Hall effect, the highest amplitude of THz-emission was registered at minimal Cobalt thickness (3 nm), which proves the criticality of the interface effects and best spin current distribution

for the effective spin-charge transformation. In Co/W structures we found a reverse dependence of THz-emission amplitude indicating a more complex generation mechanism which includes both, the super-fast demagnetization and the spin-charge transformation due to the inverse spin Hall effect. Ultimately, the study focuses on the criticality of structural and interface characteristics of ferromagnetic films for improvement of THz-emitters. This influence is most noticeable in the films of small thickness, where complex interactions at microscopic level can greatly modify the magnetic and, as a consequence, terahertz properties. Thus, our studies not only expand the understanding of fundamental physical processes in the spintronic systems, but also provide practical guidelines for improvement of their efficiency and functionality, including control of THz-emission polarization.

#### Funding

This study was supported by grant No. 21-79-10353 from the Russian Science Foundation, (<https://rscf.ru/project/21-79-10353>).

#### Conflict of interest

The authors declare that they have no conflict of interest.

#### References

- [1] T. Kampfrath, M. Battiato, P. Maldonado, G. Eilers, J. Nötzold, S. Mährlein, V. Zbarsky, F. Freimuth, Y. Mokrousov, S. Blügel, M. Wolf, I. Radu, P.M. Oppeneer, M. Münzenberg. *Nature Nanotechnol.* **8**, 256 (2013).
- [2] R. Rouzegar, A.L. Chekhov, Y. Behovits, B.R. Serrano, M.A. Syskaki, C.H. Lambert, D. Engel, U. Martens, M. Münzenberg, M. Wolf, G. Jakob, M. Kläui, T.S. Seifert, T. Kampfrath. *Phys. Rev. Appl.* **19**, 034018 (2023).
- [3] C. Bull, S.M. Hewett, R. Ji, C.-H. Lin, T. Thomson, D.M. Graham, P.W. Nutter. *APL Mater.* **9**, 090701 (2021).
- [4] D. Khushayinov, S. Ovcharenko, M. Gaponov, A. Buryakov, A. Klimov, N. Tiercelin, P. Pernod, V. Nozdrin, E. Mishina, A. Sigov, V. Preobrazhensky. *Sci. Rep.* **11**, 697 (2021).
- [5] T. Seifert, S. Jaiswal, U. Martens, J. Hannegan, L. Braun, P. Maldonado, F. Freimuth, A. Kronenberg, J. Henrizi, I. Radu, E. Beaurepaire, Y. Mokrousov, P.M. Oppeneer, M. Jourdan, G. Jakob, D. Turchinovich, L.M. Hayden, M. Wolf, M. Münzenberg, M. Kläui, T. Kampfrath. *Nature Photonics* **10**, 483 (2016).
- [6] X. Wu, H. Wang, H. Liu, Y. Wang, X. Chen, P. Chen, P. Li, X. Han, J. Miao, H. Yu, C. Wan, J. Zhao, S. Chen. *Adv. Mater.* **34**, 2204373 (2022).
- [7] C. Li, B. Fang, L. Zhang, Q. Chen, X. Xie, N. Xu, Z. Zeng, Z. Wang, L. Fang, T. Jiang. *Phys. Rev. Appl.* **16**, 024058 (2021).
- [8] X. Zhou, B. Song, X. Chen, Y. You, S. Ruan, H. Bai, W. Zhang, G. Ma, J. Yao, F. Pan, Z. Jin, C. Song. *Appl. Phys. Lett.* **115**, 182402 (2019).

- [9] X. Wang, L. Cheng, D. Zhu, Y. Wu, M. Chen, Y. Wang, D. Zhao, C.B. Boothroyd, Y.M. Lam, J.-X. Zhu, M. Battiato, J.C.W. Song, H. Yang, E.E.M. Chia. *Adv. Mater.* **30**, 1802356 (2018).
- [10] E. Rongione, S. Fragkos, L. Baringthon, J. Hawecker, E. Xenogiannopoulou, P. Tsipas, C. Song, M. Mičica, J. Mangeney, J. Tignon, T. Boulier, N. Reyren, R. Lebrun, J.-M. George, P. Le Fèvre, S. Dhillon, A. Dimoulas, H. Jaffrés. *Adv. Opt. Mater.* **10**, 2102061 (2022).
- [11] H. Park, S. Rho, J. Kim, H. Kim, D. Kim, C. Kang, M.-H. Cho. *Adv. Sci.* **9**, 2200948 (2022).
- [12] X. Chen, H. Wang, H. Liu, C. Wang, G. Wei, C. Fang, H. Wang, C. Geng, S. Liu, P. Li, H. Yu, W. Zhao, J. Miao, Y. Li, L. Wang, T. Nie, J. Zhao, X. Wu. *Adv. Mater.* **34**, 2106172 (2022).
- [13] M. Chen, Y. Wu, Y. Liu, K. Lee, X. Qiu, P. He, J. Yu, H. Yang. *Adv. Opt. Mater.* **7**, 1801608 (2019).
- [14] J. Liu, K. Lee, Y. Yang, Z. Li, R. Sharma, L. Xi, T. Salim, C. Boothroyd, Y.M. Lam, H. Yang, M. Battiato, E.E.M. Chia. *Phys. Rev. Appl.* **18**, 034056 (2022).
- [15] D. Khusyainov, A. Guskov, S. Ovcharenko, N. Tiercelin, V. Preobrazhensky, A. Buryakov, A. Sigov, E. Mishina. *Materials (Basel)*. **14**, 6479 (2021).
- [16] K. Cong, E. Vetter, L. Yan, Y. Li, Q. Zhang, Y. Xiong, H. Qu, R.D. Schaller, A. Hoffmann, A.F. Kemper, Y. Yao, J. Wang, W. You, H. Wen, W. Zhang, D. Sun. *Nature Commun.* **12**, 5744 (2021).
- [17] A. Comstock, M. Biliroglu, D. Seyitliyev, A. McConnell, E. Vetter, P. Reddy, R. Kirste, D. Szymanski, Z. Sitar, R. Collazo, K. Gundogdu, D. Sun. *Adv. Opt. Mater.* **11**, 2201535 (2023).
- [18] L. Cheng, X. Wang, W. Yang, J. Chai, M. Yang, M. Chen, Y. Wu, X. Chen, D. Chi, K.E.J. Goh, J.-X. Zhu, H. Sun, S. Wang, J.C.W. Song, M. Battiato, H. Yang, E.E.M. Chia. *Nature Phys.* **15**, 347 (2019).
- [19] G. Torosyan, S. Keller, L. Scheuer, R. Beigang, E.Th. Pappaionnou. *Sci. Rep.* **8**, 1311 (2018).
- [20] Y. Wu, M. Elyasi, X. Qiu, M. Chen, Y. Liu, L. Ke, H. Yang. *Adv. Mater.* **29**, 1603031 (2017).
- [21] T.S. Seifert, N.M. Tran, O. Gueckstock, S.M. Rouzegar, L. Nadvornik, S. Jaiswal, G. Jakob, V.V. Temnov, M. Müntzenberg, M. Wolf. *J. Phys. D* **51**, 364003 (2018).
- [22] D. Khusyainov, S. Ovcharenko, A. Buryakov, A. Klimov, P. Pernod, V. Nozdrin, E. Mishina, A. Sigov, V. Preobrazhensky, N. Tiercelin. *Phys. Rev. Appl.* **17**, 044025 (2022).
- [23] A.M. Buryakov, A.V. Gorbatova, P.Y. Avdeev, E.D. Lebedeva, K.A. Brekhov, A.V. Ovchinnikov, N.S. Gusev, E.A. Karashtin, M.V. Sapozhnikov, E.D. Mishina, N. Tiercelin, V.L. Preobrazhensky. *Appl. Phys. Lett.* **123**, 082404 (2023).
- [24] G. Lezier, P. Koleják, J.-F. Lampin, K. Postava, M. Vanwollegem, N. Tiercelin. *Appl. Phys. Lett.* **120**, 152404 (2022).
- [25] P. Agarwal, L. Huang, S.T. Lim, R. Singh. *Nature Commun.* **13**, 4072 (2022).
- [26] P. Koleják, G. Lezier, K. Postava, J.-F. Lampin, N. Tiercelin, M. Vanwollegem. *ACS Photonics* **9**, 1274 (2022).
- [27] D. Kong, X. Wu, B. Wang, T. Nie, M. Xiao, C. Pandey, Y. Gao, L. Wen, W. Zhao, C. Ruan, J. Miao, Y. Li, L. Wang. *Adv. Opt. Mater.* **7**, 1900487 (2019).
- [28] F.A. Zainullin, D.I. Khusyainov, M. V. Kozintseva, A.M. Buryakov. *Russ. Technol. J.* **10**, 74 (2022).
- [29] N. Kumar, R.W.A. Hendrikx, A.J.L. Adam, P.C.M. Planken. *Opt. Express* **23**, 14252 (2015).

*Translated by T.Zorina*